ACS SENSORS

pubs.acs.org/acssensors

Article

# Tuning the Surface Molecular Charge of Organic Photoelectrochemical Transistors with Significantly Improved Signal Resolution: A General Strategy toward Sensitive Bioanalysis

Meng-Jiao Lu, Cheng-Jun Li, Rui Ban,* Feng-Zao Chen, Jin Hu, Ge Gao, Hong Zhou,* Peng Lin, and Wei-Wei Zhao*

Cite This: *ACS Sens.* 2022, 7, 2788−2794

Read Online

ACCESS | Metrics & More | Article Recommendations | Supporting Information

**ABSTRACT:** Nature makes use of molecular charges to operate specific biological synthesis and reactions. Targeting advanced opto-bioelectronic sensors, organic photoelectrochemical transistors (OPECTs), taking advantage of the light fuel substituting an external gate potential, is now debuting and expected to serve as a universal platform for studying the rich light−biomatter interplay for new bioanalytics. Given the ubiquity of charged biomolecules in nature, molecular charge manipulation should underpin a generic route for innovative OPECT regulation and operation, which nevertheless has remained unachieved. Herein, this work manifests the biological tuning of surface charge toward the OPECT biosensor, which was exemplified by a light-sensitive CdS quantum dot (QD) gate electrode interfaced by a smart DNA superstructure with adenosine triphosphate (ATP) responsiveness. Highly negative-charged supramolecular DNA concatemers were self-assembled via sequential hybridization, and the ATP-triggered disassembly of the DNA concatemers would cause a tandem change of the effective gate voltage and transfer characteristics with significantly improved resolution. The present opto-bioelectronic device translates the events of charged molecules into amplified electrical signals and outlines a generic format for the future exploitation of rich biological tunability and light−biomatter interplay for innovative bioanalytics and beyond.

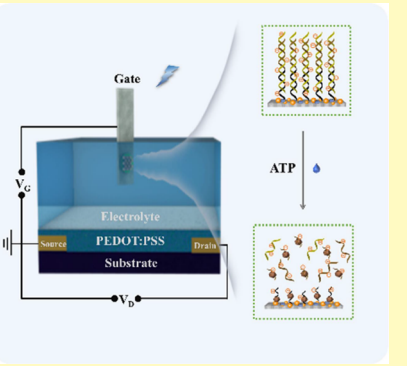


**KEYWORDS:** *organic photoelectrochemical transistor, tuning, molecular charge, DNA, effective gate voltage*



Photoelectrochemical (PEC) bioanalytics have been shown to possess desirable advantages in terms of reduced background and thus high sensitivity due to the totally separated energy forms of the input (photons) and output (electrons) signals.[1,2] To date, numerous PEC biosensors have been developed for purpose-specific applications ranging from in vivo to in vitro detection at either nanoscopic or macroscopic levels.[3−10] Nevertheless, to amplify the signals, PEC biosensors lack the essential amplification capability like transistors. That is why current PEC biosensors generally resort to various enzymatic or nucleic acid amplifications.[11−19]

Organic electrochemical transistors (OECTs), based on the modulation of channel conductivity by volumetric ionic injection from the electrolyte, have evolved as a powerful platform for advanced bioelectronics, circuits, memory, and neuromorphic devices.[20−23] Toward biosensory systems, due to its intrinsic amplification function, any bio-induced small variation of the surface potential could be magnified by the integrated potentiometric transducer into a substantially changed channel current.[24−35] Nevertheless, in addition to drain voltage ($V_D$), conventional OECT necessitates the prolonged application of gate voltage ($V_G$) that is disadvantageous for many vulnerable biomolecules[36] and could not realize the desirable photonic operation.[37,38]

In this scenario, we have pioneered the technique of organic photoelectrochemical transistors (OPECTs) based on the fusion between PEC and OECTs.[39] Replacement of the electrical input by light as the fuel could not only principally save the power supply to make the device structurally simplified but also permit the low-background, zero-gate-biased, remote-controlled, and even self-powered operation in a noncontact way.[40,41] Our recent studies further indicated the versatility of this methodology to study various light−biomatter interplays toward new opto-logic[42] and immunoassay applications.[43] Despite these progresses, the research in this arena, for example, the operation mechanism, is still quite limited due to its very short development time, and much remains to be explored.

Nature has optimized biomolecules and biosystems bearing specific charges that are capable of exquisite biological

**Received:** July 13, 2022
**Accepted:** August 29, 2022
**Published:** September 7, 2022

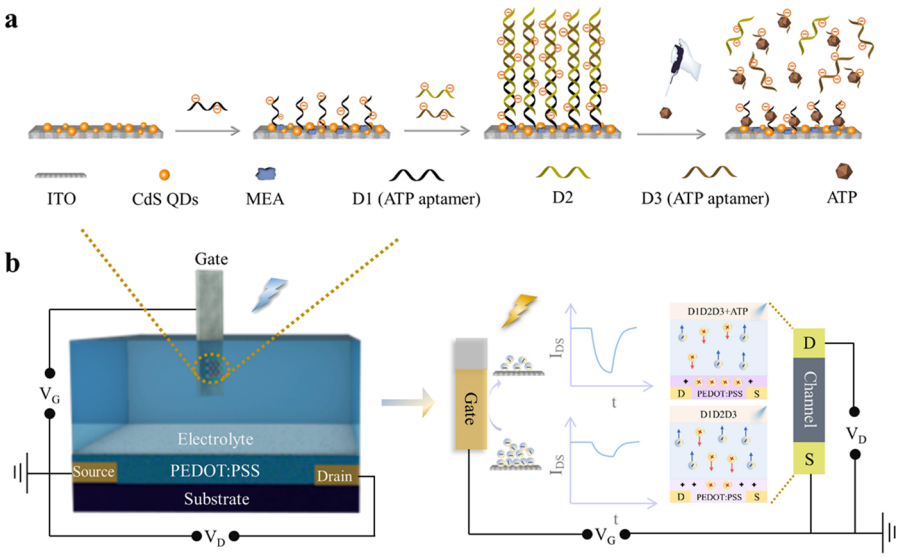


**Figure 1.** Illustration of (a) gate photoanode with DNA supersandwich assemblies. (b) Operation rationale of the system with target-tuning surface charges.

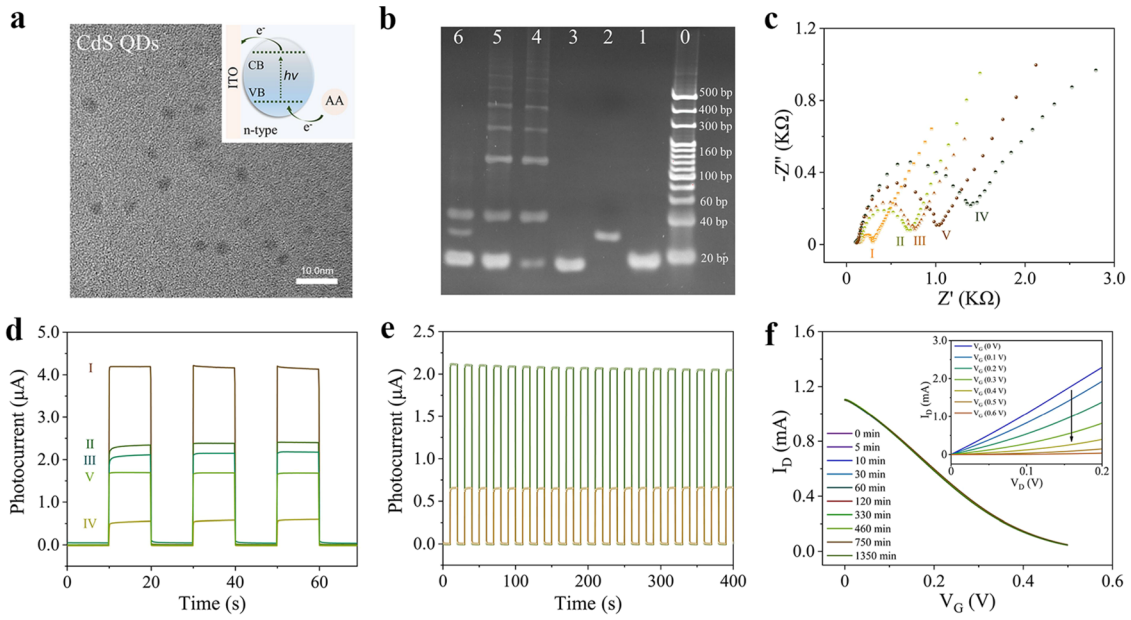


**Figure 2.** (a) TEM image of CdS QDs. Inset: Schematic of the exciton transfer route of CdS QDs upon light illumination. (b) Gel electrophoresis of seven channels corresponding to 0# (control), 1# (D1, 1.0 $\mu$M), 2# (D2, 1.0 $\mu$M), 3# (D3, 1.0 $\mu$M), 4# (D2 and D3, 1.0 $\mu$M), 5# (D1, D2, and D3, 1.0 $\mu$M), and 6# (D1, D2, D3, and ATP, with 1.0 nM ATP), respectively. (c) EIS and (d) photocurrent responses of the stepwise modification of ITO electrode: (curve I) CdS QDs/ITO electrode, (curve II) after D1 modification, (curve III) after MEA blocking, (curve IV) after D2/D3 modification, and (curve V) after treatment by 1.0 nM ATP. (e) Photocurrent responses of the as-developed electrode (orange curve) before and (green curve) after treatment by 1.0 $\mu$M ATP for 20 light off/on cycles over 400 s. (f) Long-duration stability of the transfer curves of the PEDOT:PSS device using Ag/AgCl as the gate electrode. Inset: the output curves of the device with different $V_G$.

functions. For example, positively charged stretches interact with the negatively charged ribosome walls and slow down the translation during protein expression.[44] Also, the charges of amino acids are the important driving force for tridimensional protein folding toward certain biological functions. Beyond proteins, DNA molecules are also optimized by evolution to bear negative charges, to store the genetic information, and to guide life development.[45] Inspired by the ubiquity of biomolecular charges and the relevant surface potential, we hypothesize that the rational manipulation of the charged supramolecules could underpin unique routes for OPECT-interrogating biological systems.

Herein, biologically tuning the surface charges of the OPECT biosystem was accomplished with significantly improved signal resolution, which was exemplified by a CdS quantum dot (QD)/indium tin oxide (ITO) gate electrode interfaced by flexible polyanion DNA chains with adenosine triphosphate (ATP) responsiveness (see Supporting Information for the experimental details). As depicted schematically in Figure 1, a supramolecular DNA structure, with high negative charges, was initially established on the CdS QDs/ITO gate


https://doi.org/10.1021/acssensors.2c01493
ACS Sens. 2022, 7, 2788−2794

electrode through the functionalization of 5′-aminated DNA 1 (ATP aptamers, denoted as D1) onto the carboxylated CdS QDs via amidation and the subsequent DNA self-assembly containing repeated sequences of DNA 2 (denoted as D2) and DNA 3 (ATP aptamers, denoted as D3) that were partially recognized on specific regions. The corresponding sequences are summarized in Table S1. The ATP treatment would disassemble the concatenated DNA chains and release D2 and D3, largely reducing the negative charge densities and alternating the responses of a poly(3,4-ethylenedioxythiophene):poly(styrene sulfonate) (PEDOT:PSS) channel with well-resolved transfer characteristics under light illumination. This representative system not only accomplished the target-dependent tuning of the opto-bioelectronic interface toward the model ATP detection with a low limit but also would develop as an extensible format for future OPECT regulation and operation.

## RESULTS AND DISCUSSION

As shown in Figure 2a, TEM characterization revealed that the sizes of the as-fabricated CdS QDs corresponded to ca. 3 nm, and the homogeneous distribution of the sizes would be advantageous to the development of superior photoanodes with photoexcited charge transfer, as illustrated in Figure 2a inset. Upon light illumination, CdS QDs would absorb photons with energies higher than that of their band gaps, and the corresponding photovoltaic effect stemming from the transfer of the conduction band (CB) electrons and valence band (VB) holes, respectively, to ITO and the electron donor of ascorbic acid (AA) would be equivalent to the addition of extra positive potential to $V_G$ within the configuration of OPECT.[38] Then, gel electrophoresis was implemented to study the formation of the DNA supersandwich structures, with seven channels that corresponded to 0# (control), 1# (D1), 2# (D2), 3# (D3), 4# (D2 and D3), 5# (D1, D2, and D3), and 6# (D1, D2, D3, and ATP), respectively. As shown in Figure 2b, three single ladders appeared in the channels 1#–3#, indicating the similar molecular weights of aptamers D1 and D3 and the different one of D2. The appearance of many ladders in 4# and 5# indicated the presence of various supersandwich DNA structures with different molecular weights, whereas the three ladders in 6# validated the disassembly of the supersandwich DNA structures by treatment with ATP.[46]

Figure 2c shows the stepwise change of electrochemical impedance spectroscopy (EIS) of the ITO electrode with five different modification states for the biosensor development. As shown, with the sequential modification of CdS QDs (curve I), D1 (curve II), monoethanolamine (MEA) (curve III), and sandwich DNA formation (curve IV), the gradual increase of the resistance ($R_{et}$) indicated the successful stepwise modification. Further, the enhanced $R_{et}$ value could be attributed to the nonconductive properties of DNA with negative charges, obstructing the diffusion of the negatively charged electrochemical probe to the electrode surface.[47] However, the ATP-triggered disassembly of the DNA superstructures induced the decrease of resistance (curve V), which matched well with gel electrophoresis. The development procedure was further characterized by the PEC technique. As displayed in Figure 2d, the pristine CdS QDs/ITO electrode exhibited a high photocurrent intensity of ca. 4.2 $\mu$A (curve I), which exhibited a gradual decrease to ca. 2.4 $\mu$A (curve II), ca. 2.2 $\mu$A (curve III), and finally to ca. 0.6 $\mu$A (curve IV) due to the formation of the DNA layer on the electrode. As expected, the treatment by 1.0 nM ATP induced the recovery of the photocurrent to ca. 1.7 $\mu$A (curve V). Under an optimized time of 60 min for ATP-stimulated release, as shown in Figure S1, the evolution of photocurrent in ATP detection was then recorded. Figure 2e shows the photocurrent responses of the as-developed electrode before (orange curve) and after (green curve) treatment by 1.0 $\mu$M ATP for 20 light off/on cycles over 400 s, and the barely changed signaling indicated good stability.

On the other hand, for a typical depletion-type PEDOT:PSS device, exertion of a positive $V_G$ would cause the de-doping of the polymer channel and thus the decreased channel current ($I_D$). To study the capability of $V_G$ to regulate $I_D$, the transfer characteristic was evaluated in phosphate-buffered saline (PBS) solution for 1350 min with the use of an Ag/AgCl gate. As shown in Figure 2f, good transfer characteristic was demonstrated by the obviously decreased $I_D$ with the increase of $V_G$. Moreover, the transfer curves exhibited no change from 0 to 1350 min, indicating the superior stability of the device. Figure 2f inset shows the corresponding output curves with variable $V_G$ steps of 0 to 0.6 V, revealing the $V_G$-controlled responses of $I_D$. In addition, the time-dependent $I_D$ signal output study in Figure S2 illustrated its rapid response and satisfactory signal output stability.

Next, the CdS QDs/ITO gate was coupled with the PEDOT:PSS part to test the feasibility of the proposed device, which was initially investigated by studying the transfer characteristics in the absence and presence of light illumination. As shown in Figure 3a and inset, in the dark

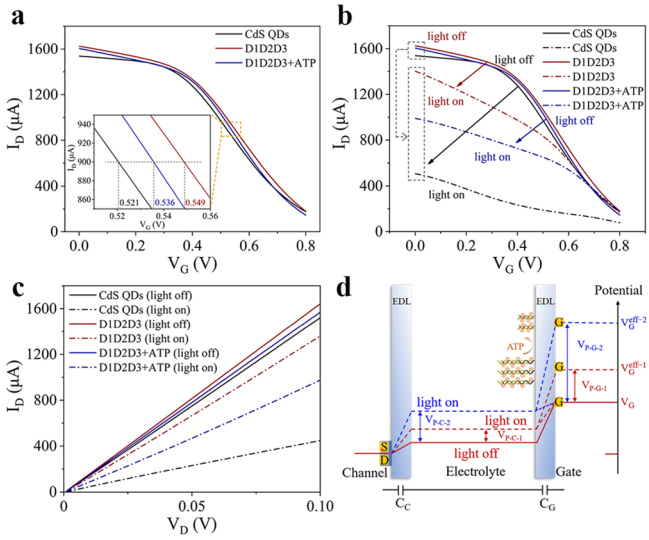


**Figure 3.** Transfer curves of the OPECT system (a) in the dark and (b) upon light illumination. (c) Corresponding output curves. (d) Evolution of the potential distributions of the proposed OPECT biosensor.

state, as compared to that of CdS QDs/ITO (black solid curve), the transfer curve shifted slightly to a higher gate voltage after the formation of the DNA superstructure (red solid curve), while the one after ATP treatment (blue solid curve) sat between the two curves due to the reduced DNA amount on the electrode surface. Such a phenomenon agreed with our previous observation in conventional OECT configuration[47] and should be attributed to the dipole


https://doi.org/10.1021/acssensors.2c01493
ACS Sens. 2022, 7, 2788−2794

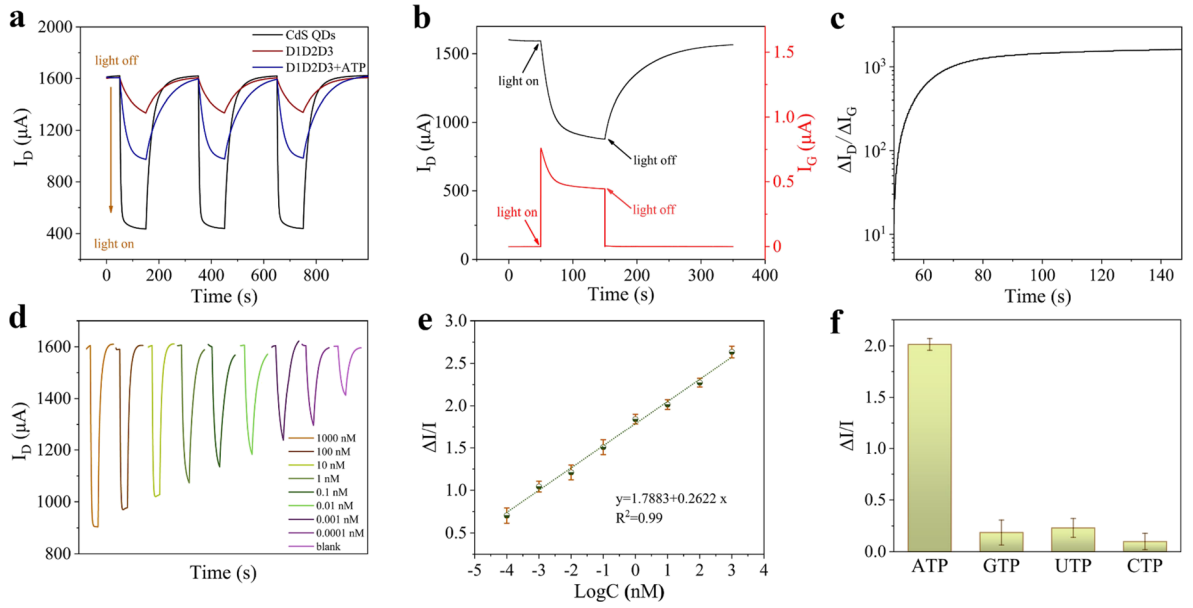


**Figure 4.** (a) Time-dependent $I_D$ responses of three repeated light on/off cycles at $V_G$ of 0 V. (b) Comparison of the transient $I_G$ (red curve) and $I_D$ (black curve) of one light on/off cycle. (c) Corresponding current gain. (d) $I_D$ signals to ATP with various concentrations and (e) derived calibration curves. (f) Selectivity study to ATP of 10 nM and GTP, UTP, and CTP of 100 nM. Error bars were derived from three repeated tests.

generated by the polyanion DNA,[48] which could be explained by eqs 1 and 2:

$$V_G^{eff} = V_G + V_{offset} \quad (1)$$

$$\Delta V_{offset} = \Delta\psi \quad (2)$$

Specifically, the effective gate voltage ($V_G^{eff}$) equated to the sum of instrumental $V_G$ and the offset voltage ($V_{offset}$), which herein was equivalent to the potential change ($\Delta\psi$) at the gate surface, where the assembly and disassembly of DNA superstructures occurred, and ($\Delta\psi$) could be given by eq 3:

$$\Delta\psi = \frac{nQ_D}{\varepsilon_r\varepsilon_0}t_D \quad (3)$$

where $n$ represents the amount of DNA molecules, $Q_D$ represents the pure charge of one DNA, $\varepsilon_r$ represents the relative dielectric constant of the DNA layer, $\varepsilon_0$ represents the dielectric permittivity of the free space, and $t_D$ is the DNA layer thickness. Therefore, the observed behaviors can be attributed to the alternation of $V_{offset}$ that is controlled by the total negative charges of DNA on the gate surface.

As shown in Figure 3b, light illumination had driven a substantial move of the transfer characteristic curves, resulting into ones with significantly improved resolution. The transfer curves of pristine CdS QDs/ITO exhibited the most prominent shift (black dotted curve), and the presence of DNA superstructures induced an obvious shift to a higher level (red dotted curve), which further decreased after ATP treatment (blue dotted curve). Figure 3c shows the corresponding output curves in the absence and presence of light illumination, which matched well with the transfer curves. Such results clearly showed the good resolution of the curves recorded under the OPECT operation and strongly indicated the possibility to perform relevant OPECT detection at zero gate bias ($V_G$ = 0 V).

Then, we discuss the underlying rationale of this OPECT biosystem. Figure 3d specifically depicts the evolution of potential distribution of the device. According to the Bernards model,[20] the two electric double layers (EDLs) associated with the two solid/liquid interfaces (i.e., gate/electrolyte and channel/electrolyte) could be treated as two series capacitors (i.e., $C_G$ and $C_C$). In the dark, the total applied potential of $V_G$ was shared by $C_G$ and $C_C$, and the corresponding potential drop of $V_{G/E}$ and $V_{C/E}$ was decided by their ratio $\gamma$ ($\gamma = C_C/C_G$) (red solid curve). Upon light illumination, for the n-type CdS QDs, the light-induced generation of photovoltage ($V_P$) was equivalent to the addition of an extra positive voltage,[41] leading to an increased $V_G^{eff-1}$ that is distributed across the two interfaces according to $\gamma$ (red dotted curve). The subsequent ATP-triggered release of DNA would decrease the surface negative charges, further generating a higher $V_G^{eff-2}$ (blue dotted curve). More specifically, at $V_G$ of 0 V and in the absence of light illumination, $PEDOT^+$ in its oxidized state guaranteed the high conductivity of the channel and thus the high $I_D$. Light illumination would facilitate the injection of cations into the channel and decrease its conductivity via the reduction of $PEDOT^+$ to $PEDOT^0$ and thus decrease $I_D$. Further decrease of the negative DNA charge would reduce the channel conductivity more and lead to a more decreased $I_D$.

In this context, varying the transition states from the ATP-dependent disassembly of DNA superstructures could result in varying residual negative charges and different $V_G^{eff}$; the OPECT biosensor could thus be achieved via tracking the $I_D$ variation ($I_{D\text{-}step}$), which was defined as the variation of $I_D$ between the absence and presence of light illumination. Note that the light-fueled generation of $I_{D\text{-}step}$ could be performed at zero gate bias ($V_G$ = 0 V) with a reduced background. Figure 4a records the corresponding stepwise transient photocurrent responses upon the intermittent light irradiation. As shown, the pristine CdS QDs/ITO electrode exhibited a high $I_{D\text{-}step}$ of ca. 1164 μA (black curve), which significantly decreased to ca. 230 μA due to the formation of the DNA superstructure (red curve). Treatment by 1.0 nM ATP induced the recovery of $I_{D\text{-}step}$ to ca. 625 μA (blue curve), which agreed well with the development of transfer curves. A relatively reproducible signal


https://doi.org/10.1021/acssensors.2c01493
ACS Sens. 2022, 7, 2788−2794

could be observed after three cycles, suggesting the good stability of the system. Figure 4b shows the $I_{D\text{-step}}$ value of ca. 680 $\mu$A and $I_{G\text{-step}}$ of ca. 0.459 $\mu$A upon treatment by 10 nM ATP. As shown in Figure 4c, a high current gain (defined as the ratio of $I_{D\text{-step}}$ with respect to $I_{G\text{-step}}$) of 3 orders of magnitude was obtained. This current gain was similar to that of our earlier reported hydrogel-based OPECT system,[43] which clearly indicated the high operation efficiency of this system and exhibited its capability for amplifying the input current.[49]

The $I_D$ responses to ATP of different concentrations are shown in Figure 4d, $I_D$ enhanced with the increasing ATP concentrations, demonstrating the ATP-controlled release of DNA and hence the enhanced de-doping of the channel, as reflected by the increased $I_{D\text{-step}}$. Figure 4e shows the corresponding linear relationship between 0.1 pM and 1.0 $\mu$M ($R^2$ = 0.99), and the detection limit was determined as 0.1 pM, which was comparable to the results of many recent reports, as listed in Table S2. The reproducibility was investigated by studying three electrodes against 0.1 pM of ATP, with RSD of 5.7%, indicating good reproducibility. Figure 4f shows the selectivity study by testing interfering species including guanosine 5′-triphosphate (GTP), uridine 5′-triphosphate (UTP), and cytidine 5′-triphosphate (CTP), the signals of which were all less than 9% of that of ATP, suggesting the acceptable selectivity.

## CONCLUSIONS

Briefly, this study has presented a new mechanism for OPECT operation based on the biological tuning of the surface charges and the corresponding regulation of $V_G^{eff}$ with well-resolved signal resolution, which was exemplified by a PEDOT:PSS device integrated with a CdS QD gate photoanode interfacing a polyanion DNA superstructure with ATP responsiveness. In this system, the ATP-triggered disassembly of the supermolecular DNA concatemers could influence the surface negative charge, inducing a tandem change of the surface potential, the channel conductivity, and the $I_D$ response. Significantly, as compared to those of conventional OECT, well-resolved transfer characteristics were obtained in this OPECT platform, and the as-developed device was successfully applied toward the detection of the model target ATP with a low limit. This study features tuning the biomolecular charges for advanced OPECT bioanalytics. Given the ubiquity of charged biomolecules in nature, this methodology is expected to serve as a generic platform for OPECT, probing various nucleic acid binding, protein recognition, or biocatalytic events, provided that the change of surface potential is appropriately induced. Future exploitation of the immense biological tunability and rich light−biomatter interplay is envisioned to yield innovative OPECT biosystems with unknown characteristics and applications.

## ASSOCIATED CONTENT

### Supporting Information

The Supporting Information is available free of charge at https://pubs.acs.org/doi/10.1021/acssensors.2c01493.

Reagents and apparatus; experimental setup and data acquisition; native polyacrylamide gel electrophoretic characterization (PAGE) analysis; OPECT device fabrication; synthesis of CdS QDs; fabrication of CdS QD-modified electrodes; DNA immobilization and hybridization; DNA sequences; time optimization of ATP-stimulated release; stability of the fabricated device; and comparison of the published methods for ATP determination (PDF)

## AUTHOR INFORMATION


### Corresponding Authors

**Rui Ban** − *School of Chemistry and Materials Science, Guizhou Education University, Guiyang 550018, China; School of Chemical Engineering, Guizhou Minzu University, Guiyang 550025, China*; Email: chem_banrui@163.com

**Hong Zhou** − *Shandong Key Laboratory of Biochemical Analysis, College of Chemistry and Molecular Engineering, Qingdao University of Science and Technology, Qingdao 266042, China*; orcid.org/0000-0002-9264-7148; Email: zhouhong@qust.edu.cn

**Wei-Wei Zhao** − *State Key Laboratory of Analytical Chemistry for Life Science, School of Chemistry and Chemical Engineering, Nanjing University, Nanjing 210023, China*; orcid.org/0000-0002-8179-4775; Email: zww@nju.edu.cn

### Authors

**Meng-Jiao Lu** − *School of Chemistry and Materials Science, Guizhou Education University, Guiyang 550018, China; School of Chemical Engineering, Guizhou Minzu University, Guiyang 550025, China; State Key Laboratory of Analytical Chemistry for Life Science, School of Chemistry and Chemical Engineering, Nanjing University, Nanjing 210023, China*

**Cheng-Jun Li** − *State Key Laboratory of Analytical Chemistry for Life Science, School of Chemistry and Chemical Engineering, Nanjing University, Nanjing 210023, China; School of Chemical Engineering, Guizhou Minzu University, Guiyang 550025, China*

**Feng-Zao Chen** − *State Key Laboratory of Analytical Chemistry for Life Science, School of Chemistry and Chemical Engineering, Nanjing University, Nanjing 210023, China*

**Jin Hu** − *State Key Laboratory of Analytical Chemistry for Life Science, School of Chemistry and Chemical Engineering, Nanjing University, Nanjing 210023, China; Shenzhen Key Laboratory of Special Functional Materials & Guangdong Research Center for Interfacial Engineering of Functional Materials, College of Materials Science and Engineering, Shenzhen University, Shenzhen 518060, China*

**Ge Gao** − *State Key Laboratory of Analytical Chemistry for Life Science, School of Chemistry and Chemical Engineering, Nanjing University, Nanjing 210023, China*

**Peng Lin** − *Shenzhen Key Laboratory of Special Functional Materials & Guangdong Research Center for Interfacial Engineering of Functional Materials, College of Materials Science and Engineering, Shenzhen University, Shenzhen 518060, China*; orcid.org/0000-0002-6154-4859

Complete contact information is available at: https://pubs.acs.org/10.1021/acssensors.2c01493


### Author Contributions

The manuscript was written through contributions of all authors.

### Notes

The authors declare no competing financial interest.



https://doi.org/10.1021/acssensors.2c01493
ACS Sens. 2022, 7, 2788−2794

## ■ ACKNOWLEDGMENTS

The authors thank the National Natural Science Foundation of China (grant nos. 21974059 and 22174063), the Science and Technology Project of Guizhou Province (ZK [2022]327), the Natural Science Foundation of Department of Education of Guizhou Province ([2021]021), the High-Level Overseas Talent Innovation and Entrepreneurship Project of Guizhou Province [(2019)11], the Natural Science Foundation of Guizhou Education University (2020BS031), and Shandong Key Laboratory of Biochemical Analysis (SKLBA2102).

## ■ REFERENCES

(1) Zhao, W. W.; Xu, J. J.; Chen, H. Y. Photoelectrochemical DNA Biosensors. *Chem. Rev.* **2014**, *114*, 7421−7441.
(2) Zhao, W. W.; Xu, J. J.; Chen, H. Y. Photoelectrochemical Bioanalysis: The State of the Art. *Chem. Soc. Rev.* **2015**, *44*, 729−741.
(3) Ruan, Y. F.; Chen, F. Z.; Xu, Y. T.; Zhang, T. Y.; Yu, S. Y.; Zhao, W. W.; Jiang, D. C.; Chen, H. Y.; Xu, J. J. An Integrated Photoelectrochemical Nanotool for Intracellular Drug Delivery and Evaluation of Treatment Effect. *Angew. Chem., Int. Ed.* **2021**, *60*, 25762−25765.
(4) Chen, F. Z.; Li, Z.; Liu, X. N.; Zhu, Y. C.; Han, D. M.; Chen, H. Y. Target-Dependent Gating of Nanopores Integrated with H-Cell: Toward A General Platform for Photoelectrochemical Bioanalysis. *Anal. Chem.* **2021**, *93*, 5001−5004.
(5) Zhou, Q.; Xue, H. J.; Zhang, Y. Y.; Lv, Y. Q.; Li, H. G.; Liu, S. Q.; Shen, Y. F.; Zhang, Y. J. Metal-Free All-Carbon Nanohybrid for Ultrasensitive Photoelectrochemical Immunosensing of alpha-Fetoprotein. *ACS Sens.* **2018**, *3*, 1385−1391.
(6) Zhang, B. H.; Wang, H.; Xi, J. J.; Zhao, F. Q.; Zeng, B. Z. Novel $Bi_{2+x}WO_6$ p-n Homojunction Nanostructure: Preparation, Characterization, and Application for a Self-Powered Cathodic Photoelectrochemical Immunosensor. *ACS Sens.* **2020**, *5*, 2876−2884.
(7) Fu, B. H.; Zhang, Z. H. Rationally Engineered Photonic-Plasmonic Synergistic Resonators in Second Near-Infrared Window for in Vivo Photoelectrochemical Biodetection. *Nano Lett.* **2019**, *19*, 9069−9074.
(8) Ye, X. X.; Wang, X.; Kong, Y.; Dai, M. J.; Han, D. X.; Liu, Z. H. FRET Modulated Signaling: A Versatile Strategy to Construct Photoelectrochemical Microsensors for in Vivo Analysis. *Angew. Chem., Int. Ed.* **2021**, *60*, 11774−11778.
(9) Qin, Y.; Wen, J.; Zheng, L. R.; Yan, H. Y.; Jiao, L.; Wang, X. S.; Cai, X. L.; Wu, Y.; Chen, G. J.; Chen, L. J.; Hu, L. Y.; Gu, W. L.; Zhu, C. Z. Single-Atom-Based Heterojunction Coupling with Ion-Exchange Reaction for Sensitive Photoelectrochemical Immunoassay. *Nano Lett.* **2021**, *21*, 1879−1887.
(10) Zhan, W. W.; Kuang, Q.; Zhou, J. Z.; Kong, X. J.; Xie, Z. X.; Zheng, L. S. Semiconductor@Metal-Organic Framework Core-Shell Heterostructures: A Case of ZnO@ZIF-8 Nanorods with Selective Photoelectrochemical Response. *J. Am. Chem. Soc.* **2013**, *135*, 1926−1933.
(11) Leng, D. Q.; Zhao, J. H.; Ren, X.; Xu, R.; Liu, L.; Liu, X. J.; Li, Y. Y.; Wei, Q. $MoSe_2$/CdSe Heterojunction Destruction by Cation Exchange for Photoelectrochemical Immunoassays with a Controlled-Release Strategy. *Anal. Chem.* **2021**, *93*, 10712−10718.
(12) Zeng, R. J.; Wang, W. J.; Cai, G. N.; Huang, Z. L.; Tao, J. M.; Tang, D. P.; Zhu, C. Z. Single-Atom Platinum Nanocatalyst-Improved Catalytic Efficiency with Enzyme-DNA Supermolecular Architectures. *Nano Energy* **2020**, *74*, No. 104931.
(13) Li, H. B.; Han, M.; Weng, X.; Zhang, Y. Y.; Li, J. DNA-Tetrahedral-Nanostructure-Based Entropy-Driven Amplifier for High-Performance Photoelectrochemical Biosensing. *ACS Nano* **2021**, *15*, 1710−1717.
(14) Zhang, Q. Q.; Fu, Y. M.; Xiao, K.; Du, C. C.; Zhang, X. H.; Chen, J. H. Sensitive Dual-Mode Biosensors for CYFRA21-1 Assay Based on the Dual-Signaling Electrochemical Ratiometric Strategy and "On-Off-On" PEC Method. *Anal. Chem.* **2021**, *93*, 6801−6807.
(15) Cui, L.; Shen, J. Z.; Li, C. C.; Cui, P. P.; Luo, X. L.; Wang, X. L.; Zhang, C. Y. Construction of a Dye-Sensitized and Gold Plasmon-Enhanced Cathodic Photoelectrochemical Biosensor for Methyltransferase Activity Assay. *Anal. Chem.* **2021**, *93*, 10310−10316.
(16) Li, L.; Zhang, Y.; Yan, Z.; Chen, M. Q.; Zhang, L. N.; Zhao, P. N.; Yu, J. H. Ultrasensitive Photoelectrochemical Detection of MicroRNA on Paper by Combining a Cascade Nanozyme-Engineered Biocatalytic Precipitation Reaction and Target-Triggerable DNA Motor. *ACS Sens.* **2020**, *5*, 1482−1490.
(17) Li, F.; Wang, S. Y.; Yin, H. S.; Chen, Y.; Zhou, Y. L.; Huang, J.; Ai, S. Y. Photoelectrochemical Biosensor for DNA Formylation Detection in Genomic DNA of Maize Seedlings Based on Black $TiO_2$-Enhanced Photoactivity of $MoS_2/WS_2$ Heterojunction. *ACS Sens.* **2020**, *5*, 1092−1101.
(18) Zhang, Q.; Zhang, L.; Liu, X. N.; Li, Z.; Li, Z.; Wu, X. M.; Wang, G. L.; Zhao, W. W. Establishing Interfacial Charge-Transfer Transitions on Ferroelectric Perovskites: An Efficient Route for Photoelectrochemical Bioanalysis. *ACS Sens.* **2020**, *5*, 3827−3832.
(19) Li, M. J.; Xiong, C.; Zheng, Y. N.; Liang, W. B.; Yuan, R.; Chai, Y. Q. Ultrasensitive Photoelectrochemical Biosensor Based on DNA Tetrahedron as Nanocarrier for Efficient Immobilization of CdTe QDs-Methylene Blue as Signal Probe with Near-Zero Background Noise. *Anal. Chem.* **2018**, *90*, 8211−8216.
(20) Rivnay, J.; Inal, S.; Salleo, A.; Owens, R. M.; Berggren, M.; Malliaras, G. G. Organic Electrochemical Transistors. *Nat. Rev. Mater.* **2018**, *3*, 17086.
(21) Wang, N. X.; Yang, A. N.; Fu, Y.; Li, Y. Z.; Yan, F. Functionalized Organic Thin Film Transistors for Biosensing. *Acc. Chem. Res.* **2019**, *52*, 277−287.
(22) Lin, P.; Yan, F. Organic Thin-Film Transistors for Chemical and Biological Sensing. *Adv. Mater.* **2012**, *24*, 34−51.
(23) Lubrano, C.; Matrone, G. M.; Iaconis, G.; Santoro, F. New Frontiers for Selective Biosensing with Biomembrane-Based Organic Transistors. *ACS Nano* **2020**, *14*, 12271−12280.
(24) Ohayon, D.; Nikiforidis, G.; Savva, A.; Giugni, A.; Wustoni, S.; Palanisamy, T.; Chen, X.; Maria, I. P.; Di Fabrizio, E.; Costa, P. M. F. J.; McCulloch, I.; Inal, S. Biofuel Powered Glucose Detection in Bodily Fluids with an N-Type Conjugated Polymer. *Nat. Mater.* **2020**, *19*, 456−463.
(25) Romele, P.; Gkoupidenis, P.; Koutsouras, D. A.; Lieberth, K.; Kovács-Vajna, Z. M.; Blom, P. W. M.; Torricelli, F. Multiscale Real Time and High Sensitivity Ion Detection with Complementary Organic Electrochemical Transistors Amplifier. *Nat. Commun.* **2020**, *11*, 3743.
(26) Guo, K.; Wustoni, S.; Koklu, A.; Díaz-Galicia, E.; Moser, M.; Hama, A.; Alqahtani, A. A.; Ahmad, A. N.; Alhamlan, F. S.; Shuaib, M.; Pain, A.; McCulloch, I.; Arold, S. T.; Grünberg, R.; Inal, S. Rapid Single-Molecule Detection of COVID-19 and MERS Antigens via Nanobody-Functionalized Organic Electrochemical Transistors. *Nat. Biomed. Eng.* **2021**, *5*, 666−677.
(27) Koklu, A.; Wustoni, S.; Musteata, V. E.; Ohayon, D.; Moser, M.; McCulloch, I.; Nunes, S. P.; Inal, S. Microfluidic Integrated Organic Electrochemical Transistor with a Nanoporous Membrane for Amyloid-Beta Detection. *ACS Nano* **2021**, *15*, 8130−8141.
(28) Tang, T.; Savva, A.; Traberg, W. C.; Xu, C.; Thiburce, Q.; Liu, H. Y.; Pappa, A. M.; Martinelli, E.; Withers, A.; Cornelius, M.; Salleo, A.; Owens, R. M.; Daniel, S. Functional Infectious Nanoparticle Detector: Finding Viruses by Detecting Their Host Entry Functions Using Organic Bioelectronic Devices. *ACS Nano* **2021**, *15*, 18142−18152.
(29) Jimbo, Y.; Sasaki, D.; Ohya, T.; Lee, S.; Lee, W.; Arab Hassani, F.; Yokota, T.; Matsuura, K.; Umezu, S.; Shimizu, T.; Someya, T. An Organic Transistor Matrix for Multipoint Intracellular Action Potential Recording. *Proc. Natl. Acad. Sci. U. S. A.* **2021**, *118*, No. e2022300118.
(30) Pappa, A. M.; Liu, H. Y.; Traberg-Christensen, W.; Thiburce, Q.; Savva, A.; Pavia, A.; Salleo, A.; Daniel, S.; Owens, R. M. Optical and Electronic Ion Channel Monitoring from Native Human Membranes. *ACS Nano* **2020**, *14*, 12538−12545.


https://doi.org/10.1021/acssensors.2c01493
*ACS Sens.* 2022, 7, 2788−2794

(31) Spyropoulos, G. D.; Gelinas, J. N.; Khodagholy, D. Internal Ion-Gated Organic Electrochemical Transistor: A Building Block for Integrated Bioelectronics. *Sci. Adv.* **2019**, *5*, No. eaau7378.
(32) Flagg, L. Q.; Bischak, C. G.; Onorato, J. W.; Rashid, R. B.; Luscombe, C. K.; Ginger, D. S. Polymer Crystallinity Controls Water Uptake in Glycol Side-Chain Polymer Organic Electrochemical Transistors. *J. Am. Chem. Soc.* **2019**, *141*, 4345−4354.
(33) van de Burgt, Y.; Melianas, A.; Keene, S. T.; Malliaras, G.; Salleo, A. Organic Electronics for Neuromorphic Computing. *Nat. Electron.* **2018**, *1*, 386−397.
(34) Ji, J. L.; Wang, H. W.; Liu, R.; Jiang, X. N.; Zhang, Q.; Peng, Y. B.; Sang, S. B.; Sun, Q. J.; Wang, Z. L. Dual-Liquid-Gated Electrochemical Transistor and Its Neuromorphic Behaviors. *Nano Energy* **2021**, *87*, No. 106116.
(35) Yang, A. N.; Li, Y. Z.; Yang, C. X.; Fu, Y.; Wang, N. X.; Li, L.; Yan, F. Fabric Organic Electrochemical Transistors for Biosensors. *Adv. Mater.* **2018**, *30*, No. e1800051.
(36) Rivnay, J.; Leleux, P.; Sessolo, M.; Khodagholy, D.; Herve, T.; Fiocchi, M.; Malliaras, G. G. Organic Electrochemical Transistors with Maximum Transconductance at Zero Gate Bias. *Adv. Mater.* **2013**, *25*, 7010−7014.
(37) Nawaz, A.; Liu, Q.; Leong, W. L.; Fairfull-Smith, K. E.; Sonar, P. Organic Electrochemical Transistors for in Vivo Bioelectronics. *Adv. Mater.* **2021**, No. 2101874.
(38) Kim, J.; Lee, H. C.; Kim, K. H.; Hwang, M. S.; Park, J. S.; Lee, J. M.; So, J. P.; Choi, J. H.; Kwon, S. H.; Barrelet, C. J.; Park, H. G. Photon-Triggered Nanowire Transistors. *Nat. Nanotechnol.* **2017**, *12*, 963−968.
(39) Song, J. J.; Lin, P.; Ruan, Y. F.; Zhao, W. W.; Wei, W. W.; Hu, J.; Ke, S. M.; Zeng, X. R.; Xu, J. J.; Chen, H. Y.; Ren, W.; Yan, F. Organic Photo-Electrochemical Transistor-Based Biosensor: A Proof-of-Concept Study Toward Highly Sensitive DNA Detection. *Adv. Healthcare Mater.* **2018**, *7*, No. 1800536.
(40) Li, Z.; Hu, J.; Gao, G.; Liu, X. N.; Wu, J. Q.; Xu, Y. T.; Zhou, H.; Zhao, W. W.; Xu, J. J.; Chen, H. Y. Organic Photoelectrochemical Transistor Detection of Tear Lysozyme. *Sens. Diagn.* **2022**, *1*, 294−300.
(41) Lu, M. J.; Chen, F. Z.; Hu, J.; Zhou, H.; Chen, G. X.; Yu, X. D.; Ban, R.; Lin, P.; Zhao, W. W. Regulating Light-Sensitive Gate of Organic Photoelectrochemical Transistor Toward Sensitive Biodetection at Zero Gate Bias. *Small Struct.* **2021**, *2*, No. 2100087.
(42) Xu, Y. T.; Li, Z.; Yuan, C.; Wu, J. Q.; Hu, J.; Lin, P.; Zhao, W. W.; Chen, H. Y.; Xu, J. J. Bipolar Modulation of the Ionic Circuit for Generic Organic Photoelectrochemical Transistor Logic and Sensor. *Adv. Optical Mater.* **2022**, *10*, No. 2102687.
(43) Hu, J.; Lu, M. J.; Chen, F. Z.; Jia, H. M.; Zhou, H.; Li, K. Z.; Zeng, X. R.; Zhao, W. W.; Lin, P. Multifunctional Hydrogel Hybrid-Gated Organic Photoelectrochemical Transistor for Biosensing. *Adv. Funct. Mater.* **2022**, *32*, No. 2109046.
(44) Di Savino, A.; Foerster, J. M.; Ullmann, G. M.; Ubbink, M. The Charge Distribution on a Protein Surface Determines Whether Productive or Futile Encounter Complexes Are Formed. *Biochemistry* **2021**, *60*, 747−755.
(45) Requiao, R. D.; Fernandes, L.; de Souza, H. J. A.; Rossetto, S.; Domitrovic, T.; Palhano, F. L. Protein Charge Distribution in Proteomes and Its Impact on Translation. *PLoS Comput. Biol.* **2017**, *13*, No. 1005549.
(46) Jiang, Y. N.; Liu, N. N.; Guo, W.; Xia, F.; Jiang, L. Highly-Efficient Gating of Solid-State Nanochannels by DNA Supersandwich Structure Containing ATP Aptamers: A Nanofluidic IMPLICATION Logic Device. *J. Am. Chem. Soc.* **2012**, *134*, 15395−15401.
(47) Lin, P.; Luo, X. T.; Hsing, I. M.; Yan, F. Organic Electrochemical Transistors Integrated in Flexible Microfluidic Systems and Used for Label-Free DNA Sensing. *Adv. Mater.* **2011**, *23*, 4035−4040.
(48) Thompson, M.; Cheran, L. E.; Zhang, M.; Chacko, M.; Huo, H.; Sadeghi, S. Label-Free Detection of Nucleic Acid and Protein Microarrays by Scanning Kelvin Nanoprobe. *Biosens. Bioelectron.* **2005**, *20*, 1471−1481.
(49) Tan, S. T. M.; Giovannitti, A.; Melianas, A.; Moser, M.; Cotts, B. L.; Singh, D.; McCulloch, I.; Salleo, A. High-Gain Chemically Gated Organic Electrochemical Transistor. *Adv. Funct. Mater.* **2021**, *31*, No. 2010868.




https://doi.org/10.1021/acssensors.2c01493
*ACS Sens.* 2022, 7, 2788−2794